



This is a repository copy of *Design and synthesis of fused pyridine building blocks for automated library generation*.

White Rose Research Online URL for this paper:
<https://eprints.whiterose.ac.uk/168909/>

Version: Accepted Version

Article:

Harrity, J.P.A. orcid.org/0000-0001-5038-5699, Mora-Radó, H., Czechtizky, W. et al. (1 more author) (2021) Design and synthesis of fused pyridine building blocks for automated library generation. *ChemMedChem*, 16 (2). pp. 328-334. ISSN 1860-7179

<https://doi.org/10.1002/cmdc.202000852>

This is the peer reviewed version of the following article: Harrity, J..P., Mora-Radó, H., Czechtizky, W. and Méndez, M. (2020), Design and Synthesis of Fused Pyridine Building Blocks for Automated Library Generation. *ChemMedChem*, which has been published in final form at <https://doi.org/10.1002/cmdc.202000852>. This article may be used for non-commercial purposes in accordance with Wiley Terms and Conditions for Use of Self-Archived Versions.

Reuse

Items deposited in White Rose Research Online are protected by copyright, with all rights reserved unless indicated otherwise. They may be downloaded and/or printed for private study, or other acts as permitted by national copyright laws. The publisher or other rights holders may allow further reproduction and re-use of the full text version. This is indicated by the licence information on the White Rose Research Online record for the item.

Takedown

If you consider content in White Rose Research Online to be in breach of UK law, please notify us by emailing eprints@whiterose.ac.uk including the URL of the record and the reason for the withdrawal request.



eprints@whiterose.ac.uk
<https://eprints.whiterose.ac.uk/>

Design and Synthesis of Fused Pyridine Building Blocks for Automated Library Generation

Helena Mora-Radó,^[a] Werngard Czechtizky,^[b,c] María Méndez,^{*[b]} and Joseph P. A. Harrity^{*[a]}

[a] Dr. H. Mora-Radó, Prof. J. P. A. Harrity
Department of Chemistry, University of Sheffield
Sheffield, S3 7HF (U.K.)
E-mail: j.harrity@sheffield.ac.uk

[b] Dr. W. Czechtizky, Dr. M. Méndez
Integrated Drug discovery, R&D, Sanofi Aventis Deutschland GmbH, Industriepark Höchst, D-65926 Frankfurt Am Main, Germany.

[c] Present address: Respiratory, Inflammation, Autoimmunity IMED Biotech Unit, AstraZeneca, Gothenburg, Sweden.

Supporting information for this article is given via a link at the end of the document.

Abstract: We demonstrate that a diboration-electrocyclization sequence provides access to a range of pyridine fused small molecule boronic ester building blocks, and that these are amenable to high throughput synthesis leading to biaryl and ether linked compound libraries. Moreover, the implementation of an integrated physchem and ADME profiling workflow allows accelerated design of novel lead compounds for application in drug discovery projects.

Introduction

Up to the 1990s, failure of drug candidates was mostly driven by inappropriate pharmacokinetic (PK) parameters and lack of clinical efficacy.^[1] In 2000, the attrition rate due to poor PK profiles was significantly reduced, while failure due to lack of efficacy and drug safety remained high.^[2] One of the main reasons for this reduction was the improvement of physicochemical and eADME (early compound absorption, distribution, metabolism and excretion) profiles in the course of lead optimization.^[3] Indeed, it is now common for compound optimization workflows to include the early experimental assessment of intestinal absorption (e.g. CaCo-2 profiling), inhibition of CYP3A4 enzyme, metabolic lability in microsome preparations (metabolic lability), solubility and log D.

The Integrated Drug Discovery unit at Sanofi routinely uses library synthesis to access sufficiently large compound pools to expedite the optimization of the overall profiles in a chemical series with respect to biological activity and physicochemical and eADME properties.^[4] In order to enable this approach, robust methods that permit rapid access to functionalized small molecule scaffolds is essential.^[5]

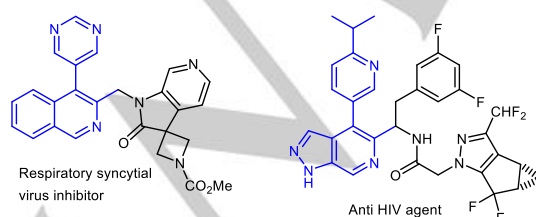
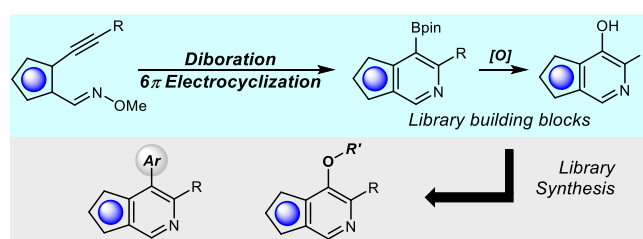


Figure 1. Bioactive (hetero)isoquinolines.

We recently highlighted how a pyrazole trifluoroborate scaffold can be easily elaborated to a series of tricycles that are subject to high-throughput experimentation with rapid testing in an integrated physicochemical and ADME profiling workflow.^[6] Isoquinolines are common motifs in pharmaceutically active compounds,^[7] and therefore broad variations of these structural motifs could represent a valuable approach to sampling the chemical space around this privileged scaffold thereby leading to promising starting points for medicinal chemistry optimization programs. In particular, 3,4-disubstituted isoquinolines and heteroisoquinolines have been disclosed that exhibit promising antiviral properties (Figure 1).^[6] A robust access to variations of these motifs would offer a valuable way to quickly support the synthesis of analogs, however, there are relatively few strategies available to prepare congested fused pyridine derivatives bearing useful functionality.^[9] We report herein the generation and characterization of a library of 3,4-substituted isoquinolines and related analogs by functionalization of organoboron intermediates that were readily accessed via our previously reported sequential Pt-catalyzed diborylation reaction and a disrotatory 6π -electrocyclic transformation (Scheme 1).^[10] Using the powerful chemistry of organoboron compounds,^[11] these building blocks can be transformed to a diverse product set, and assessed for their physicochemical and eADME properties allowing a quickly understanding of the property distribution among this chemical class and potentially expediting future medicinal chemistry programs.



Scheme 1. Divergent strategy to pyrazole-based tricycles.

Results and Discussion

Our first goal was to generate a series of boronic ester building blocks using simple and scalable chemistry. Therefore, we employed commercially available unsaturated β -bromo

FULL PAPER

aldehydes to produce a small family of yne-ene-oxime ethers via Sonogashira coupling and condensation with methoxylamine hydrochloride (further details are contained within the Supporting Information). Following diboration-electrocyclization, we were able to rapidly generate eight 3,4-disubstituted isoquinoline and isoquinoline-like scaffolds with three distinct cores and several substituents in high yield. In addition, intermediates **3**, **4**, and **6** were oxidized with hydrogen peroxide to provide the corresponding 3-hydroxypyridines **9-11**, thereby offering an alternative vector for further functionalization (Scheme 2).

Library synthesis – Generation of structural diversity and Compound Properties.

We next carried out the Suzuki coupling of boronates **1,2,5,7** and **8** in a parallel library synthesis approach using a selection of 43 different aryl bromides. In a first step, the reaction conditions for the coupling were optimized; the highest yield and broadest reagent scope was achieved using a 2nd generation S-phos precatalyst in combination with K₃PO₄ in THF.^[12,13] In total, we generated >100 novel compounds that were characterized by NMR spectroscopy and LC-MS analysis, and subsequently subjected these to our automated physicochemical and eADME profiling to acquire logD, solubility, CaCo, CYP inhibition and metabolic liability data.

Scheme 2. Library building block synthesis.

Detailed physicochemical and ADME data for all synthesized compounds are provided in the Supporting Information, but Table 1 highlights the data for those compounds that showed solubilities of >10 mg/mL at pH 7.4. The approach provided a diverse set of compounds with an attractive range of molecular weights and logD values spanning from 0 to 5. Whereas the cell permeability (CaCo-2 measurements) was generally good, the metabolic liability of most analogs in human microsomes was generally high; only 12 of the compounds shown in Table 1 exhibited values below 40%. Not surprisingly, these 12 compounds contain mostly polar substituents, which would be expected to increase metabolic stability. Finally, a significant proportion of compounds showed acceptable CYP inhibition values with IC₅₀ values >30.0 μM, albeit boronates **2** and **5** gave rise to derivatives that were more prone to CYP inhibition liability. The poor metabolic profile of derivatives of **2** is likely due to the presence of the alkene moiety, although this could be offset by employing this as a handle for the introduction of more drug-like fragments. Generally speaking, while the overall profile was dependent on the nature of both coupling partners, we found that those compounds derived from 2-pyridones **xiii** and **xiv** showed the best overall profile, with low metabolic liability, high CaCo, no CYP3A4 inhibition and reasonable logD values accompanied by a high solubility.

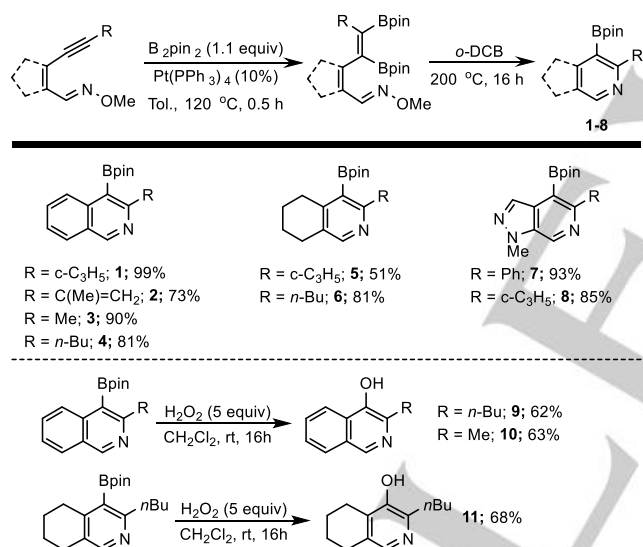
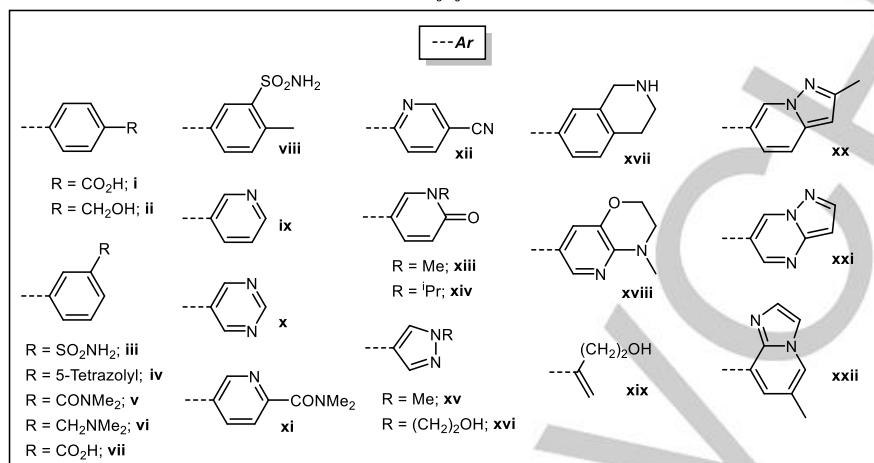
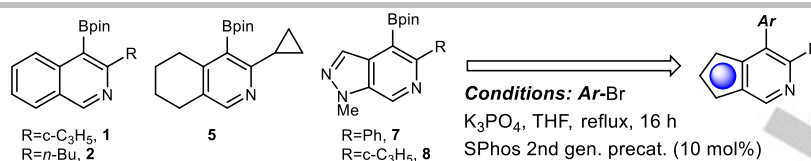


Table 1. Physical and ADME properties of a biaryl library



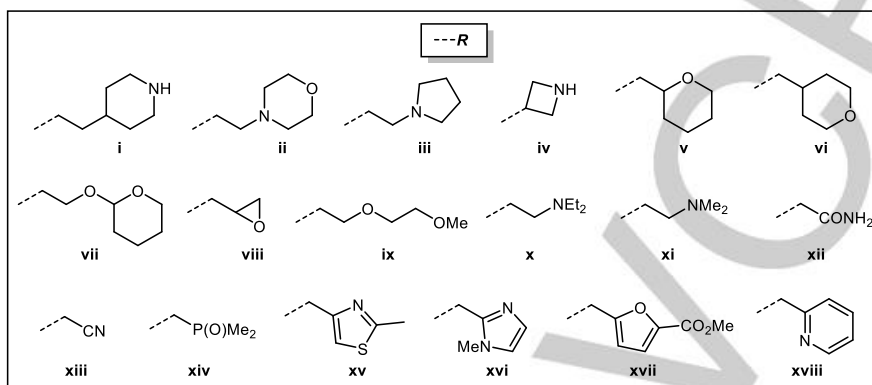
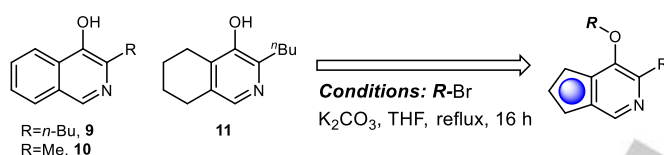
Product ^[a]	Mol. Wt.	Metabolic Lability ^[b]	CaCo-2 ^[c]	CYP inhibition ^[d]	Solubility ^[e]	logD ^[f]	Product ^[a]	Mol. Wt.	Metabolic Lability ^[b]	CaCo-2 ^[c]	CYP inhibition ^[d]	Solubility ^[e]	logD ^[f]
1iii	324.4	20	151.8	>30.0	55	2.03	2xx	299.4	85	285.2	>30.0	>1665	1.77
1iv	313.7	36	25.3	2.9	>392	0.84	2xxii	299.4	98	152.1	19.8	>230	1.74
1v	316.4	87	291.6	>30.0	187	2.41	5i	293.4	6	137.5	>30.0	>604	1.39
1xiii	276.3	5	280.8	>30.0	>1809	1.07	5ii	279.4	91	127.4	24.6	14	2.53
1ix	246.3	80	330.3	1.3	50	2.09	5v	320.4	98	183.0	>30.0	>1560	2.49
1x	247.3	77	414.9	10.2	>2022	1.35	5vi	420.5	96	92.4	>30.0	>1189	2.21
1xi	317.4	72	437.1	>30.0	>1575	1.48	5ix	250.4	96	252.8	1.9	>1997	2.15
1xiv	304.4	33	337.2	>30.0	>1643	2.02	5x	251.3	90	257.4	15.6	107	1.40
1xv	249.2	65	365.8	>30.0	>2006	1.81	5xii	275.4	83	245.7	>30.0	166	2.49
1xix	239.3	97	190.3	>30.0	>2089	1.73	5xiii	280.4	21	201.9	>30.0	>1783	1.11
1xx	300.4	68	292.2	>30.0	37	2.40	5xvii.TFA	418.5	44	52.6	27.6	179	1.31
2ii	275.4	89	139.7	>30.0	59	1.79	5xx	304.4	97	276.9	25.8	23	2.46
2v	316.4	92	194.7	27.8	>1580	1.79	7i	329.4	5	NoVal	>30.0	>1518	0.64
2vi.TFA	416.5	94	134.2	>30.0	>1201	1.52	7v	356.4	68	253.4	23.9	>1403	1.26
2viii	337.4	68	194.5	21.7	36	2.41	7vii	329.4	6	102.8	>30.0	>1518	0.91
2ix	246.3	82	243.4	<1.0	34	1.43	7xiv	344.4	36	206.9	>30.0	>1452	0.91
2xvi	279.4	35	162.6	>30.0	>282	0.40	7xxi	326.4	62	202.4	9.9	168	0.97
2xvii.TFA	414.4	23	64.8	16.9	>1207	0.72	8v	320.4	56	218.4	>30.0	>1561	1.21
2xviii	317.4	92	189.4	15.3	7	2.42	8xiv	308.4	36	196.7	>30.0	>1621	0.85
2xix	239.3	79	193.1	20.2	>2089	1.21	8xxi	290.3	62	232.5	>30.0	54	0.83

[a] Products are a biaryl consisting of the heteroaromatic fragment (**1**, **2**, **5**, **7**, **8**) bonded to the residues **i-xxii**; [b] Metabolic lability in human microsomes; Total Metabolism (%) after 30 min, no CYP inhibitor added. [c] CaCo-2; Mean; PTotal (A2B) (10^{-7} cm/s). [d] CYP inhibition, IC_{50} (INH) (μM), Isoform: CYP3A4, Substrate: Midazolam. [e] Solubility (pH 7.4; mg/mL). [f] LogD (pH 7.4), Mean. NoVal: Insufficient sample to perform the assay in this case

Our next step was to compare the physicochemical properties of our fused pyridine cores coupled to more sp^3 -rich fragments through an ether linkage. Accordingly, we alkylated phenols **9-11** with a library of alkyl bromides and our results are summarized in Table 2, again highlighting only those compounds that had solubilities of >10 mg/mL at pH 7.4.^[13]

In comparison to the biaryl derivatives of the previous libraries, the ether linked series generally provided compounds with good solubility and lower logD. However, the metabolic lability of this compound library was significant across the series with only **10i**

and **10xvi** showing reasonable metabolic stability. This was unsurprising given the number of methylene groups present in these molecules. CaCo values were overall acceptable to good with a few exceptions. CYP inhibition could be influenced by the residues linked via the ether, and this appeared to have little correlation to logD values. Finally, this library was also able to deliver intermediates with handles for further elaboration by incorporating epoxide (**9viii**) and acetal (**11vii**) fragments, as well as free amines (**9-11i**, **11iv**).

Table 2. Physical and ADME properties of an ether library

Product ^[a]	Mol. Wt.	Metabolic Lability ^[b]	Caco-2 ^[c]	CYP inhibition ^[d]	Solubility ^[e]	logD ^[f]	Product ^[a]	Mol. Wt.	Metabolic Lability ^[b]	Caco-2 ^[c]	CYP inhibition ^[d]	Solubility ^[e]	logD ^[f]
9i.TFA	426.5	51	NoVal	17.2	>1172	1.03	10xvii	297.3	100	2.0	>30.0	137	1.88
9viii	257.3	100	6.8	13.6	>1943	2.56	11i.TFA	430.5	82	35.8	4.6	>1161	1.15
9x	300.5	90	135.1	>30.0	>1664	2.00	11ii	318.5	100	165.1	4.8	1310	2.46
9xi	272.4	79	129.3	>30.0	>1836	1.42	11iii	302.5	100	103.1	>30.0	808	1.40
9xii	258.3	98	138.1	>30.0	>1936	0.85	11iv	374.4	88	NoVal	<1.0	702	0.43
9xiii	240.3	90	163.3	>30.0	>2081	2.62	11v	303.5	99	160.5	12.5	150	4.35
9xv	312.4	97	NoVal	5.7	192	3.22	11vi	303.5	99	161.8	12.9	281	3.69
9xvi	295.4	100	198.5	5.0	>1693	1.71	11vii	333.5	99	149.3	5.8	139	4.22
10i.TFA	384.4	20	45.5	>30.0	>1301	-0.11	11xii	262.4	98	NoVal	>30.0	935	1.02
10ii	272.4	47	NoVal	>30.0	>1834	0.63	11xiii	244.3	100	182.0	28.6	210	2.88
10ix	261.3	71	198.3	>30.0	>1913	0.89	11xiv	295.4	99	116.7	>30.0	314	1.07
10xii	216.2	44	144.4	>30.0	>2312	-0.55	11xv	316.5	100	172.0	5.7	299	3.45
10xiii	198.2	80	239.8	>30.0	>2522	0.69	11xvi	299.4	100	174.4	2.0	>1670	1.91
10xv	270.4	82	NoVal	>30.0	>1849	1.40	11xvii	343.4	100	2.5	>30.0	41	3.69
10xvi	253.3	36	170	12.8	>1974	0.22	11xviii	296.4	100	158.4	6.0	393	3.16

[a] Products consist of the heteroaromatic fragment (9-11) bonded to the residues i-xviii through an ether linkage; [b] Metabolic lability in human microsomes; Total Metabolism (%) after 30 min, no CYP inhibitor added. [c] CaCo-2; Mean; PTotal (A2B) (10⁻⁷ cm/s). [d] CYP inhibition, IC₅₀ (INH) (μM), Isoform: CYP3A4, Substrate: Midazolam. [e] Solubility (pH 7.4; mg/mL). [f] LogD (pH 7.4), Mean. NoVal: Insufficient sample to perform the assay in this case.

In order to better illustrate the property distribution across both compound series, we performed the analysis depicted in Figure 2. In these graphs, the physicochemical properties (Chart 1) and the eADME properties (Chart 2) are depicted as a function of molecular weight and logD, and these are provided for all synthesized compounds (including those with poorer solubilities that are described in the Supporting Information). The various fused pyridine scaffolds are represented by different colors and the shape and size of the dots indicate the different properties and their value ranges respectively. For example, for the Chart 1, the size of the points indicates the solubility range, with larger points indicating those with higher solubilities. On Chart 2, the size of the points indicates the metabolic lability in human microsomes; in this case more stable compounds are represented by larger dots. Additionally, in this chart, the shape of the points indicates the permeability in Caco2 cells: whereas low permeability is

represented with points, high permeability compounds are represented with crosses.

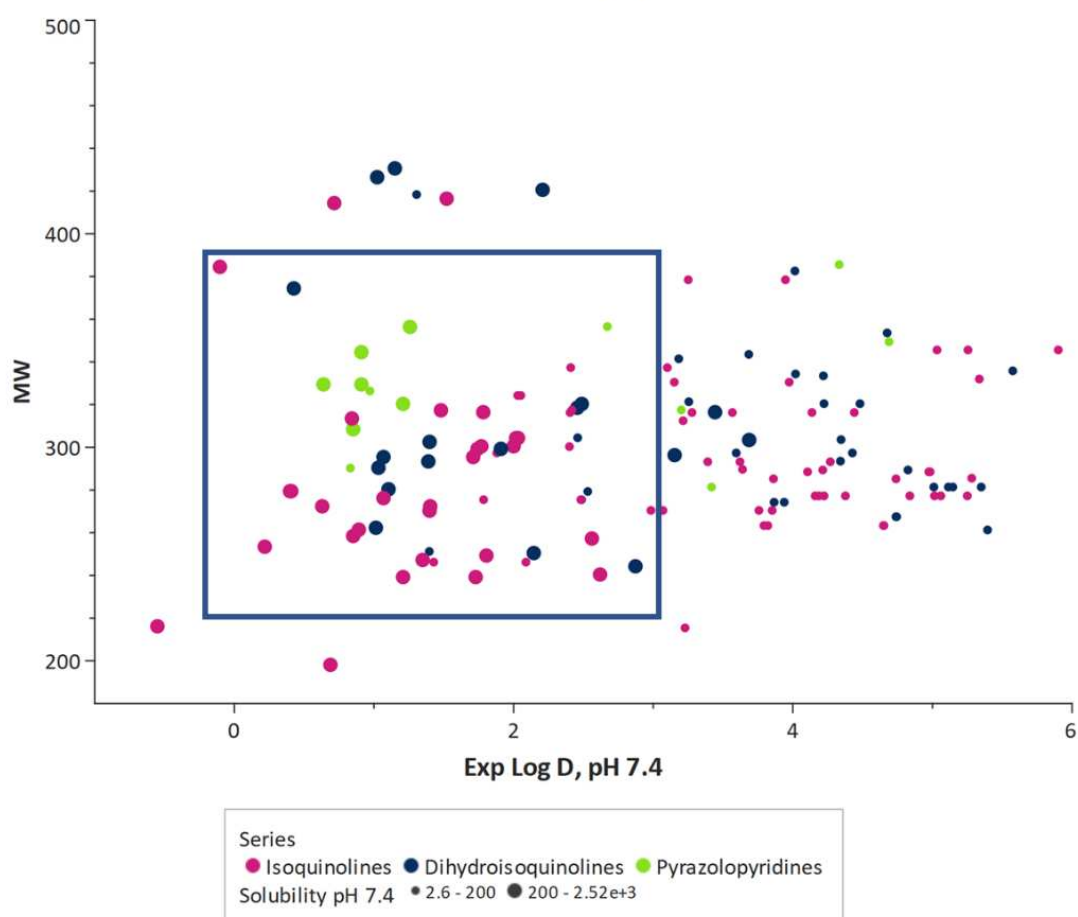
This analysis shows that all scaffolds produced compounds within the desirable range of logD (<3) and solubility (> 200 μM) (Compounds within the blue square).^[14] Although the number of compounds with acceptable metabolic stability (i.e. < 40%) is limited (larger crosses on chart 2, Figure 2), the fact that these compounds are distributed among all scaffolds and include both types of linkages (C and O) indicates, that by choosing the appropriate derivatization, the physicochemical and ADME properties of these compounds can be successfully modulated into a region of interest from a medicinal chemistry perspective. In this regard, the synthesized compounds provide potentially interesting starting points for medicinal chemistry optimization programs in the future, which could quickly expand this chemical space by using the synthetic workflow established in this study.^[15]

FULL PAPER

It is also important to note, that the heteroaromatic pyrazolo[3,4-c]pyridine core bearing this substitution pattern is underrepresented in the patent literature and a robust access to

this drug-like core and its derivatization using this methodology could provide a competitive advantage for the generation of IP.

Chart 1: MW vs Exp LogD, pH 7.4



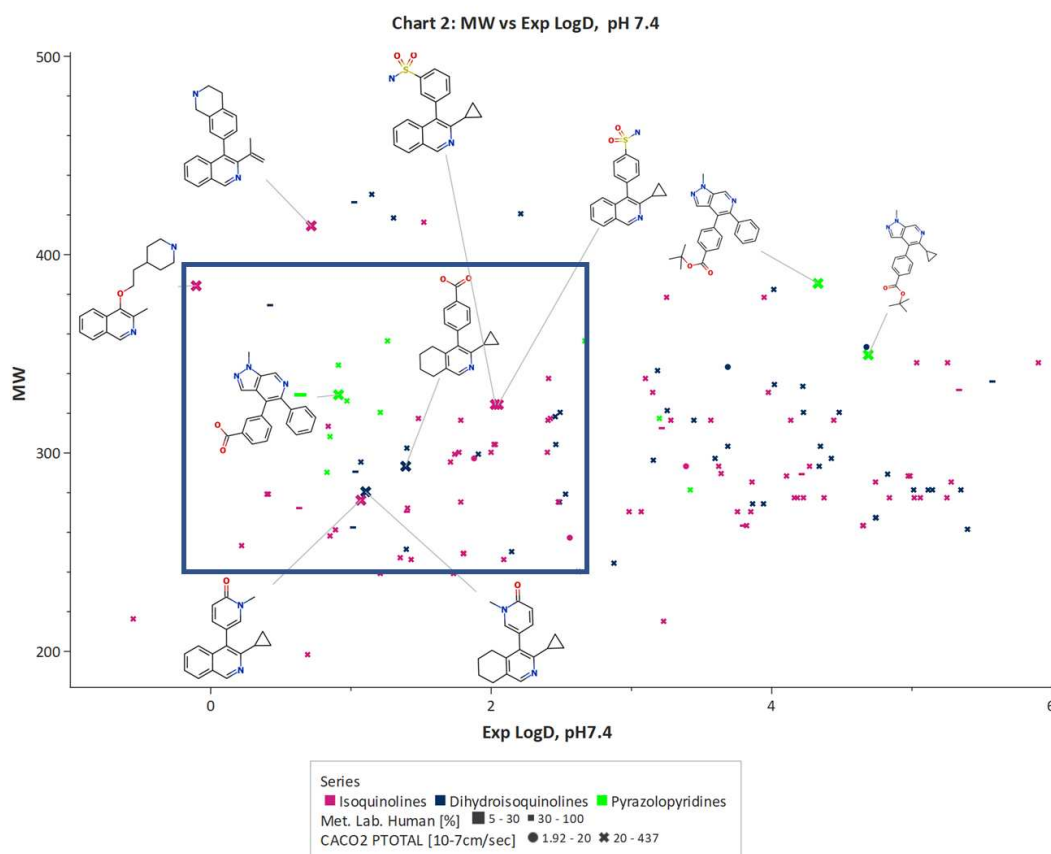


Figure 2. Representation of property distribution for all synthesized compounds according to series. Chart 1: Solubility [μM]; Chart 2: Metabolic lability [human, % metabolized] and Caco-2 Permeability [P_{total} , [$\cdot 10^{-7}$ cm/sec].

Conclusion

In conclusion, we have successfully established an efficient access to broadly modifiable fused pyridine boronates from easily accessible starting materials. Using automated parallel library synthesis, we have demonstrated the potential of these heterocyclic boronate building blocks to rapidly generate diverse compound libraries. Using Sanofi's internal compound profiling workflow, we have identified points for diversification in these compound series which give access to improved physicochemical and eADME properties.

Experimental Section

General. Characterization and synthetic procedures for compounds **1**, **2**, **5**, **7**, **8** are reported elsewhere.^[10(b),(c)]

General procedure A: Pt-catalyzed diborylation of alkynes. B_2Pin_2 (1.1 equiv) was added to a stirred solution of alkyne (1.0 equiv) in toluene (0.1 M). $\text{Pt}(\text{PPh}_3)_4$ (10 mol%) was added and the reaction was heated at 120°C for 30 min. The reaction mixture was allowed to cool to room temperature and the solvent was evaporated. The residue was purified by flash column chromatography on florisil eluting with petroleum ether (40/60) and ethyl acetate to afford the corresponding boronic esters.

General procedure B: Electrocyclization reaction of diborylalkenes.

A sealed tube containing a solution of diborylalkene in 1,2-dichlorobenzene (0.1 M) was stirred at 200°C for 16 h. The reaction mixture was allowed to cool to room temperature and was filtered through silica gel. The residue was purified by flash column chromatography on silica gel eluting with petroleum ether (40/60) and ethyl acetate to afford the corresponding isoquinolines.

General procedure C: Oxidation of boronic esters.

To a stirred solution of the aromatic boronate in dichloromethane (0.1 M) was slowly added a 30% (w/v) aqueous solution of hydrogen peroxide (1.5 equiv). The reaction was then stirred at room temperature over 24 h. Water was added and the organic layer was extracted with dichloromethane. The organic phase was dried over anhydrous MgSO_4 , filtered and the solvent was removed *in vacuo*. The residue was purified by flash column chromatography on silica gel eluting with petroleum ether (40/60) and ethyl acetate to afford the desired products.

3-methyl-4-(4,4,5,5-tetramethyl-1,3,2-dioxaborolan-2-yl)isoquinoline

(3). Following general procedure A, *E*-2-(prop-1-yn-1-yl)benzaldehyde *O*-methyl oxime (4.2 g, 24.3 mmol), B_2Pin_2 (6.8 g, 26.7 mmol) and $\text{Pt}(\text{PPh}_3)_4$ (754 mg, 0.6 mmol) in toluene (250 mL) afforded the desired product as a dark brown foam (10.3 g, 99%). ^1H NMR (400 MHz, CDCl_3): δ 8.13 (s, 1H), 7.87 (dd, $J = 8.0, 1.5$ Hz, 1H), 7.29 (td, $J = 7.5, 1.5$ Hz, 1H), 7.20 (td, $J = 7.5, 1.0$ Hz, 1H), 7.03 (dd, $J = 8.0, 1.0$ Hz, 1H), 3.94 (s, 3H), 1.53 (s, 3H), 1.33 (s, $J = 7.8$ Hz, 12H), 1.20 (s, $J = 1.0$ Hz, 6H), 1.20 (s, 6H); ^{13}C NMR (101 MHz, CDCl_3): δ 148.1, 142.1, 129.4, 129.3, 128.8, 126.4, 125.2, 83.8, 83.7, 61.8, 24.9 (x2 C), 24.8, 24.6 (x2 C); ^{11}B NMR (128 MHz, CDCl_3): δ 30.1 (br); FTIR: ν_{max} 2978 (m), 1517 (w), 1473 (m), 1332 (s).

FULL PAPER

1271 (s), 1144 (s), 1054 (m); HRMS calculated for $C_{23}H_{35}^{11}B_2NO_5$ (MH^+): 428.2774. Found: 428.2782. Following general procedure B, using *E*-2-(1,2-bis(4,4,5,5-tetramethyl-1,3,2-dioxaborolan-2-yl)prop-1-en-1-yl) benzaldehyde *O*-methyl oxime (10.8 g, 25.3 mmol) in 1,2-dichlorobenzene (250 mL) afforded the desired product as a dark orange foam (6.1 g, 90%). 1H NMR (400 MHz, $CDCl_3$): δ 9.15 (s, 1H), 8.15 (d, $J = 8.5$ Hz, 1H), 7.88 (d, $J = 8.0$ Hz, 1H), 7.64 (ddd, $J = 8.5, 7.0, 1.5$ Hz, 1H), 7.49 (t, $J = 7.5$ Hz, 1H), 2.83 (s, 3H), 1.47 (s, 12H); ^{13}C NMR (101 MHz, $CDCl_3$): δ 156.9, 153.3, 139.7, 130.5, 128.1, 126.6, 126.1, 126.0, 84.3, 25.0, 24.6; ^{11}B NMR (128 MHz, $CDCl_3$): δ 32.3 (br); FTIR: ν_{max} 2976 (m), 1574 (m), 1454 (m), 1324 (m), 1133 (s); HRMS calculated for $C_{16}H_{20}^{11}BNO_2$ (MH^+): 270.1659. Found: 270.1665.

3-*n*-butyl-4-(4,4,5,5-tetramethyl-1,3,2-dioxaborolan-2-yl)isoquinoline

(4). Following general procedure A, *E*-2-(hex-1-yn-1-yl)benzaldehyde *O*-methyl oxime (2.2 g, 10.2 mmol), B_2Pin_2 (2.91 g, 11.2 mmol) and $Pt(PPh_3)_4$ (635 mg, 0.51 mmol) in toluene (100 mL) afforded the desired product as a dark orange oil (4.63 g, 97%). 1H NMR (400 MHz, $CDCl_3$): δ 8.15 (s, 1H), 7.85 (dd, $J = 8.0, 1.5$ Hz, 1H), 7.28 (dt, $J = 7.5, 1.5$ Hz, 2H), 7.19 (td, $J = 7.5, 1.0$ Hz, 1H), 7.01 (dd, $J = 8.0, 1.0$ Hz, 1H), 3.93 (s, 3H), 1.97 – 1.88 (m, 2H), 1.34 (s, 12H), 1.24 – 1.20 (m, 2H), 1.19 (s, 12H), 1.13 – 1.07 (m, 2H), 0.71 (t, $J = 7.5$ Hz, 3H); ^{13}C NMR (101 MHz, $CDCl_3$): δ 148.3, 142.3, 129.5, 129.2, 129.1, 126.3, 125.0, 83.7 (x2 C), 61.7, 32.8, 31.0, 25.0 (x2 C), 24.7 (x2 C), 24.6 (x2 C), 22.8 (x2 C), 13.8; ^{11}B NMR (128 MHz, $CDCl_3$): δ 31.9 (br); FTIR: ν_{max} 2977 (m), 1599 (w), 1467 (m), 1307 (s), 1146 (s), 1055 (s); HRMS calculated for $C_{26}H_{41}^{11}B_2NO_5$ (MH^+): 470.3244. Found: 470.3259. Following general procedure B, using *E*-2-(1,2-bis(4,4,5,5-tetramethyl-1,3,2-dioxaborolan-2-yl)hex-1-en-1-yl) benzaldehyde *O*-methyl oxime (4.3 g, 9.2 mmol) in 1,2-dichlorobenzene (90 mL) afforded the desired product as a dark orange oil (2.32 g, 81%). 1H NMR (400 MHz, $CDCl_3$): δ 9.18 (s, 1H), 8.11 (d, $J = 8.5$ Hz, 1H), 7.87 (d, $J = 8.0$ Hz, 1H), 7.66 – 7.60 (m, 1H), 7.48 (t, $J = 7.5$ Hz, 1H), 3.10 – 3.04 (m, 2H), 1.81 – 1.71 (m, 2H), 1.46 (s, 12H), 1.45 – 1.38 (m, 2H), 0.94 (t, $J = 7.5$ Hz, 3H); ^{13}C NMR (101 MHz, $CDCl_3$): δ 160.8, 153.3, 139.8, 130.5, 128.1, 126.7, 126.1 (x 2C), 84.3, 38.5, 33.8, 25.0, 23.0, 14.1; ^{11}B NMR (128 MHz, $CDCl_3$): δ 32.3 (br); FTIR: ν_{max} 2976 (m), 1574 (m), 1454 (m), 1324 (m), 1133 (s); HRMS calculated for $C_{19}H_{26}^{11}BNO_2$ (MH^+): 312.2129. Found: 312.2136.

3-*n*-butyl-4-(4,4,5,5-tetramethyl-1,3,2-dioxaborolan-2-yl)-5,6,7,8-tetrahydroisoquinoline

(6). Following general procedure A, *E*-2-(hex-1-yn-1-yl)-1-cyclohexenecarboxaldehyde *O*-methyl oxime (3.9 g, 17.6 mmol), B_2Pin_2 (5.0 g, 19.4 mmol) and $Pt(PPh_3)_4$ (658 mg, 0.53 mmol) in toluene (170 mL) directly afforded the title product as a pale orange oil (4.5 g, 81%). 1H NMR (400 MHz, $CDCl_3$): δ 8.17 (s, 1H), 2.80 – 2.71 (m, 4H), 2.66 (br, 2H), 1.79 – 1.73 (m, 4H), 1.67 – 1.60 (m, 2H), 1.41 – 1.35 (m, 14H), 0.91 (t, $J = 7.5$ Hz, 3H); ^{13}C NMR (101 MHz, $CDCl_3$): δ 161.9, 150.5, 150.1, 129.0, 84.1, 38.5, 33.4, 29.0, 26.5, 25.0, 23.0, 22.8, 22.5, 14.1; ^{11}B NMR (128 MHz, $CDCl_3$): δ 32.2 (br); FTIR: ν_{max} 2930 (w), 1560 (m), 1475 (w), 1303 (m), 1138 (s); HRMS calculated for $C_{19}H_{30}^{11}BNO_2$ (MH^+): 316.2442. Found: 316.2452.

3-*n*-butylisoquinolin-4-ol

(9). Following general procedure C, 3-*n*-butyl-4-(4,4,5,5-tetramethyl-1,3,2-dioxaborolan-2-yl)isoquinoline (2.8 g, 9.0 mmol) and H_2O_2 (377 mg, 11.1 mmol) in dichloromethane (90 mL) afforded the desired product as a pale yellow foam (1.1 g, 62%). 1H NMR (400 MHz, $CDCl_3$): δ 8.78 (s, 1H), 8.28 (d, $J = 8.5$ Hz, 1H), 7.89 (d, $J = 8.0$ Hz, 1H), 7.65 (dd, $J = 8.0$ Hz, 1H), 7.54 (dd, $J = 8.0$ Hz, 1H), 2.99 – 2.94 (m, 2H), 1.72 – 1.63 (m, 2H), 1.30 – 1.20 (m, 2H), 0.78 (t, $J = 7.5$ Hz, 3H); ^{13}C NMR (101 MHz, $CDCl_3$): δ 146.8, 141.0, 139.1, 129.9, 129.4, 128.4, 127.3, 126.9, 121.5, 31.4, 31.3, 22.7, 13.9; FTIR: ν_{max} 2917 (m), 1586 (m), 1493 (m), 1359 (s), 1104 (s); HRMS calculated for $C_{13}H_{15}NO$ (MH^+): 202.1226. Found: 202.1230.

3-methylisoquinolin-4-ol

(10). Following general procedure C, 3-methyl-4-(4,4,5,5-tetramethyl-1,3,2-dioxaborolan-2-yl)isoquinoline (6.0 g, 22.3 mmol) and H_2O_2 (1.1 g, 33.4 mmol) in dichloromethane (225 mL) afforded the desired product as a brown foam (2.3 g, 63%). 1H NMR (400 MHz,

$CDCl_3$): δ 8.83 (s, 1H), 8.10 (d, $J = 8.5$ Hz, 1H), 7.91 (d, $J = 8.0$ Hz, 1H), 7.70 – 7.65 (m, 1H), 7.58 – 7.53 (m, 1H), 2.67 (s, 3H); ^{13}C NMR (101 MHz, $CDCl_3$): δ 146.1, 141.5, 133.5, 130.4, 128.4, 128.2, 127.4, 127.1, 120.9, 17.3; FTIR: ν_{max} 3190 (br), 2530 (br), 1542 (m), 1412 (m), 1377 (m), 1088 (s); HRMS calculated for $C_{10}H_9NO$ (MH^+): 160.0757. Found: 160.0757.

3-*n*-butyl-5,6,7,8-tetrahydroisoquinolin-4-ol

(11). Following general procedure C, 3-*n*-butyl-4-(4,4,5,5-tetramethyl-1,3,2-dioxaborolan-2-yl)-5,6,7,8-tetrahydroisoquinoline (3.4 g, 10.8 mmol) and H_2O_2 (550 mg, 16.2 mmol) in dichloromethane (110 mL) afforded the desired product as a pale orange foam (1.5 g, 68%). 1H NMR (400 MHz, $CDCl_3$): δ 7.82 (s, 1H), 2.76 – 2.72 (m, 2H), 2.71 – 2.63 (m, 4H), 1.84 – 1.71 (m, 4H), 1.62 (tt, $J = 8.0, 6.5$ Hz, 2H), 1.38 – 1.28 (m, 2H), 0.88 (t, $J = 7.5$ Hz, 3H); ^{13}C NMR (101 MHz, $CDCl_3$): δ 150.4, 146.3, 138.3, 135.3, 131.9, 31.6, 31.1, 26.2, 24.9, 24.6, 23.4, 22.8, 13.9; FTIR: ν_{max} 2931 (w), 2507 (br), 1595 (m), 1358 (m), 1207 (s), 1100 (s); HRMS calculated for $C_{13}H_{19}NO$ (MH^+): 206.1539. Found: 206.1543.

Acknowledgements

We are grateful for support from Sanofi Aventis, and the FP7 Marie Curie Actions of the European Commission (via the ITN COSSHNET network).

Keywords: ADME • boron • compound libraries • physicochemical • pyridines

- [1] R. A. Prentis, Y. Lis, S. R. Walker, *Br. J. Clin. Pharmacol.* **1988**, *25*, 387.
- [2] I. Kola, J. Landis, *Nat. Rev. Drug Discov.* **2004**, *3*, 711.
- [3] L. Di, E. H. Kerns, *Curr. Opin. Drug Discov. Devel.* **2005**, *8*, 495.
- [4] For an introduction to ADME Profiling see Chapter 13 in *Small Molecule Medicinal Chemistry: Strategies and Technologies*, K. Mertsch; M. Will; W. Czechtizky, N. Griesang, A. Marker, J. Olsen, *John Wiley & Sons, Inc.*, **2015**.
- [5] For an overview on the impact of enabling technologies on medicinal chemistry programs see: A. Vasudevan, A.R. Bogdan, H.F. Koolman, Y. Wang, S.W. Djuric, *Progress in Medicinal Chemistry*, **2017**, *56*, 1.
- [6] P. Fricero, L. Bialy, W. Czechtizky, M. Méndez, J. P. A. Harrity, *ChemMedChem* **2020**, *15*, 1634.
- [7] A search of the SciFinder® database revealed that there are more than 100 patents published containing the term 'isoquinoline' or 'dihydroisoquinoline' and their uses as therapeutics or pesticides.
- [8] (a) S. Ayesa, J. Bylund, K. Ersmark, L. Salvador Oden, F. Sehgelmeble, WO2018038667; (b) S. Babu, M. Belema, J. A. Bender, C. Iwuagwu, J. F. Dadow, S. Kumaravel, P. Nagalaskshmi, B. N. Naidu, M. Patel, K. M. Peese, R. Rajamani, M. Saulnier, A. X. Wang, WO 2018203235.
- [9] (a) H. Wang, C. Grohmann, C. Nimphius, F. Glorius, *J. Am. Chem. Soc.* **2012**, *134*, 19592; (b) S. P. J. T. Bachollet, J. F. Vivat, D. C. Cocker, H. Adams, J. P. A. Harrity, *Chem. Eur. J.* **2014**, *20*, 12889; (c) B. Su, J. F. Hartwig, *Angew. Chem. Int. Ed.* **2018**, *57*, 10163.
- [10] (a) M. P. Ball-Jones, J. Tyler, H. Mora-Radó, W. Czechtizky, M. Mendez, J. P. A. Harrity, *Org. Lett.* **2019**, *21*, 6821; (b) H. Mora-Radó, L. Sotorrios, M. P. Ball-Jones, L. Bialy, W. Czechtizky, M. Mendez, E. Gomez-Bengoia, J. P. A. Harrity, *Chem. Eur. J.* **2018**, *24*, 9530; (c) H. Mora-Radó, L. Bialy, W. Czechtizky, M. Mendez, J. P. A. Harrity, *Angew. Chem. Int. Ed.* **2016**, *55*, 5834.
- [11] *Boronic Acids: Preparation and Applications in Organic Synthesis, Medicine and Materials*, 2nd ed.; D. G. Hall, WILEY-VCH, Weinheim, 2011; Vol. 1.
- [12] T. Kinzel, Y. Zhang, S. L. Buchwald, *J. Am. Chem. Soc.* **2010**, *132*, 14073.
- [13] Reaction yields are provided in the Supporting Information. Reactions carried out in parallel were not optimized individually (for example reaction time). Instead, we employed a general method that allows the generation of the most diverse set of compounds. Individual optimization

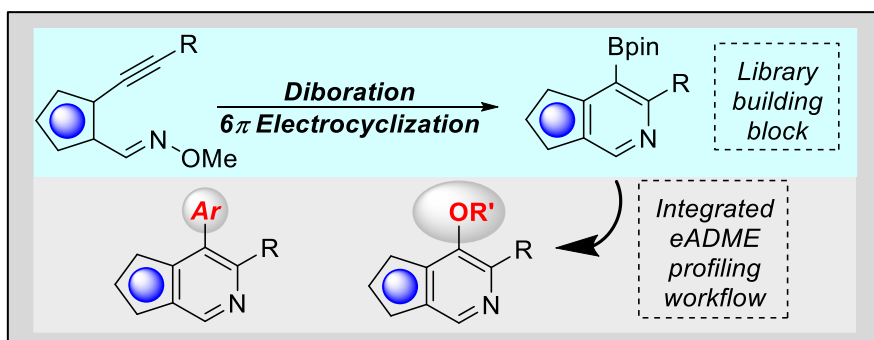
FULL PAPER

is carried out at a later stage if the compounds obtained are moved forward to the next stage of the program.

- [14] For a perspective on drug and lead likeness see C.A. Lipinski; *Drug Discovery Today:Technologies*, **2004**, 1, 337 and references therein.
- [15] *Lead Optimization for Medicinal Chemist, Pharmacokinetic Properties of Functional Groups and Organic Compounds*, Z.Dorwald, WILEY-VCH, Weinheim, 2012.

WILEY-VCH

Entry for the Table of Contents



Multiple choice! Pyridine fused boronic ester building blocks are accessible on multigram scale through a diboration-electrocyclization sequence. These are amenable to the high throughput synthesis of biaryl and ether linked compound libraries bearing a broad range of physicochemical and eADME properties.